Vol. 02, Iss. 4 (2024) 279-287, DOI: 10.61552/JME.2024.04.006

Journal of Materials and Engineering

www.jme.aspur.rs

Research article

Ixora Coccinea Extract for Biosynthesis of Titanium Dioxide Nanoparticles: A Precursor for Organic Electronics

Sunday Balogun[a], Hakeem Oyeshola[b,*], Sefiu Bello[a], Samuel Ojo[a]

[a]*Department of Materials Science and Engineering, Kwara State University, Malete, Nigeria,*
[b]*Ladoke Akintola University of Technology, Faculty of Pure and Applied Science: Ogbomoso, Oyo State, Nigeria.*

Keywords:

Ixora coccinea flower
Extract
Titanium dioxide nanoparticles
Spectroscopic characterization
Energy band gap
Microscopic characterization

* Corresponding author:

Hakeem Oyeshola
E-mail: hooyeshola@lautech.edu.ng

Received: 30 March 2024
Revised: 26 April 2024
Accepted: 31 May 2024

A B S T R A C T

This study explores the synthesis, characterization, and evaluation of titanium dioxide nanoparticles (TiO_2NPs) as a precursor for the electron transport layer in organic electronics. Traditional physical and chemical synthesis methods are not environmentally friendly or economical, due to the use of toxic chemicals and high energy. However, biosynthesis offers a low-cost, eco-friendly alternative. The synthesized NPs were characterized using various techniques, including X-ray diffraction technique, transmission electron microscopy, scanning electron microscopy, Fourier Transform Infra-red microscopy, electron dispersive X-ray, and UV-visible spectroscopy with a four-point probe equipped with Keithley2400 source meter. Results showed high crystallinity and a band gap energy of 4.02 eV. Electrical properties show sheet resistance, resistivity and conductivity as 67.22 x 10^6 Ω, 1.71 x 10^6 Ωm^{-1} and 0.585 x10^{-6} Sm^{-1} respectively which were promising, with better photovoltaic characteristics than pure titanium dioxide. These properties suggest potential applications as an electron transport layer for solar cell technology.

© 2024 Journal of Materials and Engineering

1. INTRODUCTION

The world today craves promising, economical, and clean energy for optoelectronics, photovoltaic cells and wearable electronics. Advancements in nanotechnology can be harnessed to stabilize and improve the performance of existing devices such as solar cells, photovoltaic cells, and optical devices on the nanoscale for large-area fabrication. Interlayer and window layers such as the hole transport layer or electron transport layer can be incorporated into an active layer on the nanoscale to improve the light-harvesting mechanism. Devices such as polymer solar cells made of cheap and abundant material suffer stability and flaws as a result recombination of holes and electrons. This leads to energy conversion loss These flaws make the commercialization of polymer lag behind other

solar cells. One of the methods to enhance the improvement of the performance is to introduce a photo-layer in the form of a hole transport layer or electron transport layer to suppress or mitigate the recombination of hole and electron. Metallic oxide nanoparticles can serve to suppress or hinder the recombination of hole-electron pairs. Metal oxide like Titanium dioxide (TiO_2) is a semiconductor material for optoelectronics and electronic device technologies [1-6]. Pure-state titanium dioxide (TiO_2) displays n-type semiconductor conductivity and flaws in its photocatalytic applications and metal-ion composition which must be mitigated. TiO_2 has good optical properties and a band gap (= 3.2 eV) at room temperature. TiO_2 has high dye absorption ability and excellent light scattering properties. Its properties also include chemical stability, low cost and non-toxic. To overcome the inherent flaws of TiO_2, one of the methods is to reduce the metal ions with plant extract which is the biogenic reduction of metal ions. The biosynthetic method using plant extract is a viable and simple alternative to chemical synthetic and physical methods [7-9]. Most plant extracts due to their phytochemical contents can act as capping and reducing agents in metals and metal oxides NPs [10-16]. Titanium dioxide nanoparticles have been widely studied for applications in medicine, biomedical drug delivery and pharmaceutical [17]. Synthesis of nanoparticles technologies are classified into three physical, chemical and biosynthesis [18-27]. It is, therefore, of interest to study the influence of flower extract of the Ixora coccinea plant as a reducing agent. Ixora coccinea flower was utilized as source of natural dye to fabricate dye sensitized solar cells (DSSCs) using TiO_2 electrodes revealed conversion efficiency of 1.18% [28]. This paper presents the used extract of Ixora coccinea which can bind to titanium dioxide surface to synthesize TiO_2 nanoparticles a precursor and its possible application in solar cells as an electron transport layer to prevent recombination of electrons. Synthesized titanium dioxide nanoparticles were characterized with X-ray diffractometer (XRD) (Rigaku Machine), ultraviolet–visible spectroscopy (UV-VIS) (Analytik Jena AG), Scanning Electron Microscopy (SEM) (JOEL-JSM 7600F), and Transmission Electron Microscopy (TEM) (JEM-ARM200F-G), Elemental Dispersive X-ray (EDX), Fourier transform infrared spectroscopy ((M530 FT-IR). Electrical properties were determined using a four-point probe (4PP) equipped with Keithley2400 SMU for current-voltage measurement.

2. MATERIALS AND METHODS

2.1 Materials

Titanium (IV) oxide Nanopowder (<.35nm), 97% was procured from Sigma-Aldrich**.** Other materials such as reagent ethanol, acetone, methanol, Isopropyl alcohol (lPA), hydrochloric acid (HCI), de-ionized water and Whatman filter papers were purchased locally.

2.2 Extraction procedure of Ixora coccinea plant flower

Ixora coccinea plant flowers were harvested from the environment directly. 30 g of the fresh flower of the Ixora coccinea plant harvested were thoroughly washed with clean water and de-ionized water several times to remove dirt and dried in a room for 25 days under ambient temperature.

15.0 g of dried flower of Ixora coccinea plant measured was poured into a cleaned beaker containing 70 ml of absolute ethanol (99.8%) and covered with foil for 24 h to extract the pigment. Filtration of the solution was carried out using Whatman filter papers severally to remove impurities. The filtered solution was kept for further use.

2.3 Synthesis of Titanium (IV) nanoparticles

15.0 g of Titanium (IV) oxide was dissolved in a beaker containing 30 ml of extract and stirred continuously with a magnetic stirrer for 5 h without heat for a homogenous mixture to form nanoparticles. The precipitates were filtered and washed with distilled water to remove residue. The resulting product was dried and annealed at 500 ℃ for 1 h in a furnace and left to cool in the furnace. An annealing temperature of 500 ℃ was chosen based on published studies on TiO_2 thin film [29-31]. The obtained dried coarse product of TiO_2 nanoparticles was crushed into fine powder. To make TiO_2 film over a clean glass slide substrate, TiO_2 nanoparticles were dissolved in ethanol and deposited by spin-coating technique on the glass substrate surface at 3000 rpm for 30 seconds. The thickness of the film depended on the number of drops which resulted in a thick film of TiO_2 nanoparticles. TiO_2 NP film was then annealed for 20 min at

100 ℃ to remove residual organic chemicals and impurities and the thin film was then characterized.

2.4 Characterization of TiO_2NPs

The crystal structure of synthesized TiO_2NPs was determined using XRD (Rigaku Machine). Chemical bonds and absorption bands were obtained with FT- infrared spectrophotometer (BUK model M530). Optical properties were studied with a UV-Vis spectrophotometer (model: ASUV-6300PC). The surface morphology images were viewed using a Scanning Electron Microscope (Model JOEL-JSM 7600F). Electron dispersive X-ray was utilized to determine purity and the elemental composition of prepared TiO_2NPs.

3. RESULTS AND DISCUSSION

3.1 Optical properties

Figure 1 shows the absorbance graph of synthesized TiO_2 nanoparticles. Noticeable maximum absorption peaks occurred at 250 nm to 300 nm in the solar wavelength spectrum in Figure 1. Although, absorption was noticeable at the wavelength of 250 to 350 nm. The absorption of TiO_2 nanoparticles with bulk size was observed at 350 nm which was much higher when compared to the absorption of TiO_2 nanoparticles at 250 nm to 300 nm in the wavelength spectrum. The absorption peak that occurred at 260 nm can be related to the inter-band transition on the metal electron from the basic level of the valence band.

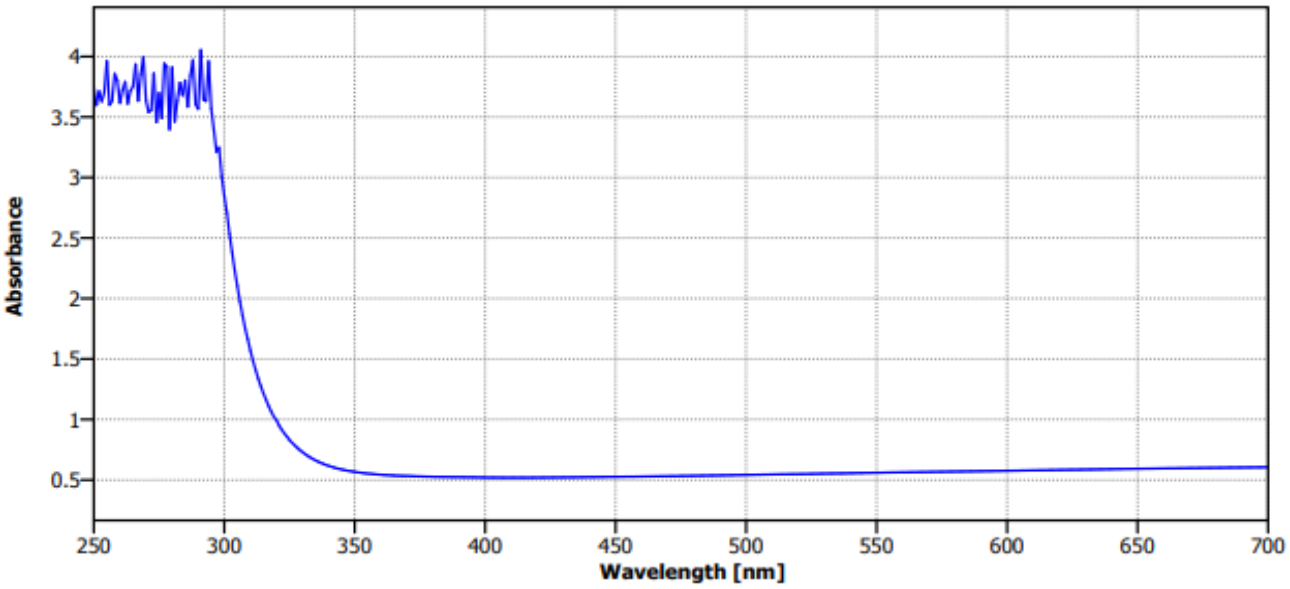


Fig. 1. Absorbance graph of synthesized TiO_2NPs.

3.1.1. Energy band gap

Optical band gap is expressed by Tauc's plot model for semiconducting materials [32] Absorption coefficient (α) was calculated with Eq. (1) assuming the film reflectance is negligible.

$$\alpha = 2.303\left(\frac{A}{t}\right) \quad (1)$$

Where α is absorption coefficient, A is absorbance, t is thickness of film. Davis & Mott's Equation (2) [33, 34] was used to calculate values to plot the graph in Figure 2.

$$(\alpha h\nu) = A(h\nu - Eg)^n \quad (2)$$

Where α is absorption coefficient, hν is photon energy, A is empirical constant, Eg is energy band gap, n = 1 and 4 for direct and indirect energy band gap respectively. Band gap energy is determined by plotting values of $(\alpha h\nu)^2$ against extrapolating linear portion of the tauc's plot to photon energy (hν) axis where $(\alpha h\nu)^2 = 0$. Mathematically, TiO_2NPs band gap energy was obtained through the graphic relation of hν and $(\alpha h\nu)^2$ photo-catalytic process takes place with the absorption of photons which excites an electron from the valence band which is full of electrons to the conduction band which was initially empty, leaving a hole in the valence band. When electron transited from the valence band to the conduction band directly it is said to be a direct transition. The optical band gap energy of TiO_2NPs from tauc plot is 4.02 eV. This result concurs with previous published articles [3, 35].

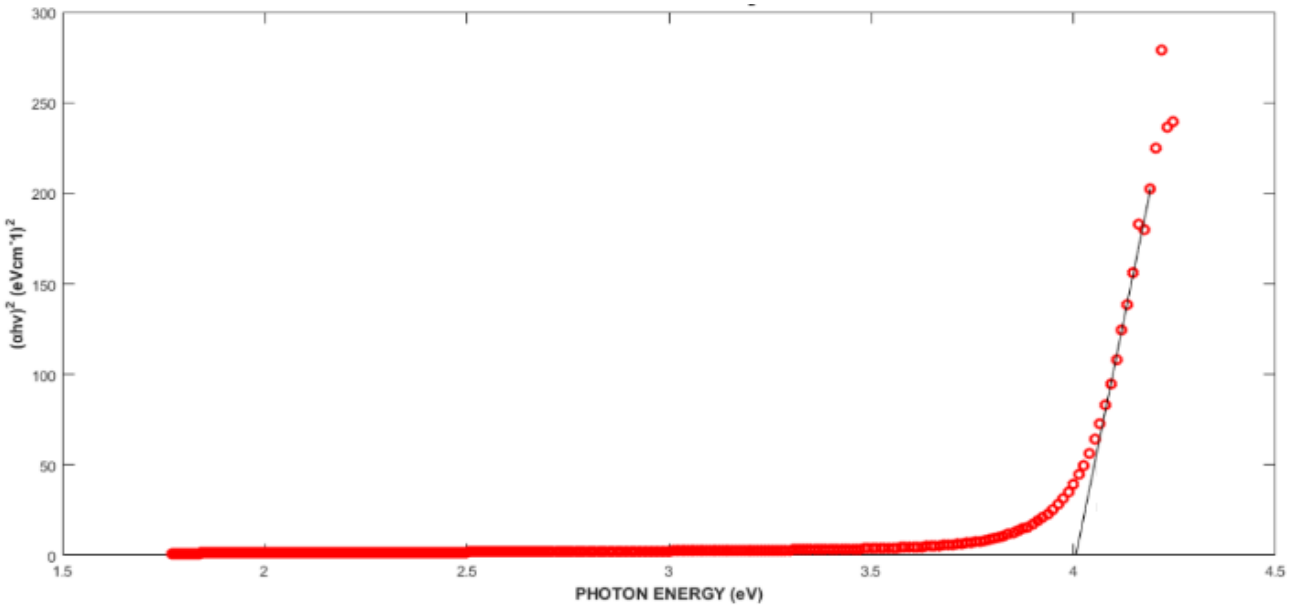


Fig. 2. Tauc's plot of band gap energy of the TiO_2 nanoparticles.

3.2 Fourier transform infrared spectroscopy analysis

Absorption peaks, functional group and chemical bonds were revealed in synthesized TiO_2NPs by FTIR Spectroscopy as shown in figure 3. The synthesized NPs peak at lower wavenumber confirmed the presence of Ti-O stretching bond. The result shows NPs exhibited bond at wavenumber 565.28 cm^{-1} assigned to the Ti-O, Ti-O-Ti vibrational single stretching bond, 1637.13 cm^{-1} depicts C= O double bond stretching modes, absorption peak at 3458.57 cm^{-1} is attributed to single bond O-H. Chemical bond confirmed the formation of TiO_2NPs.

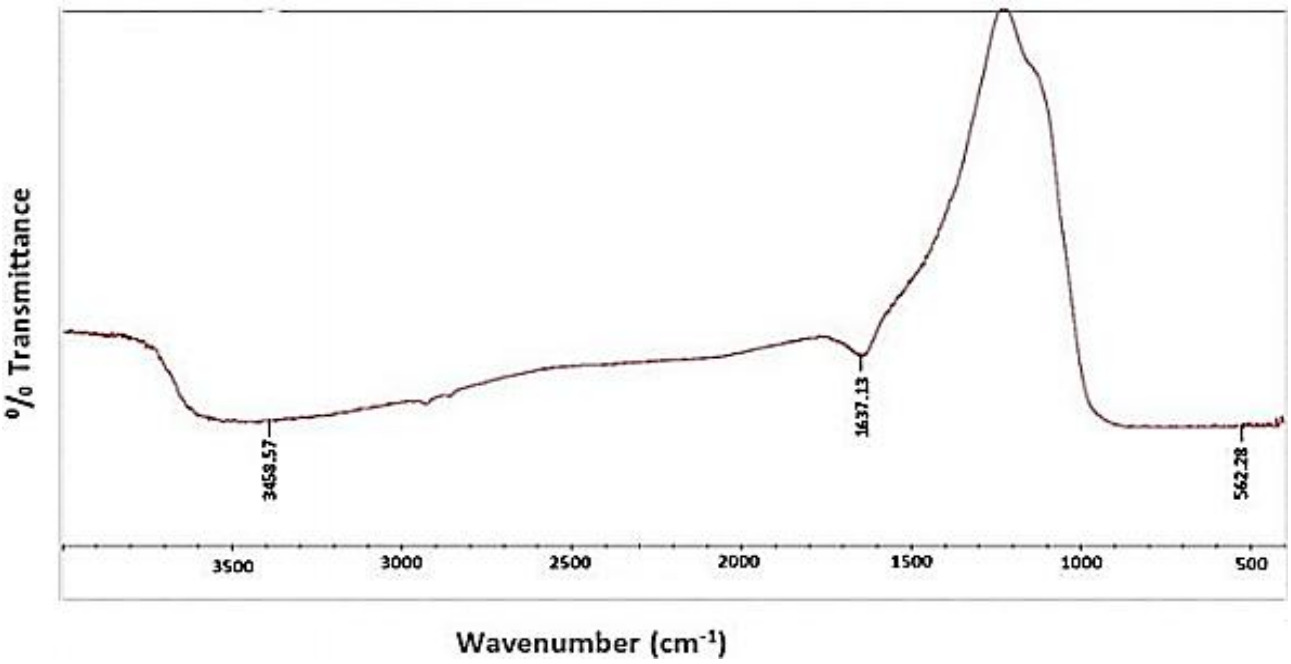


Fig. 3. FTIR Spectra of TiO_2NPs.

3.3 Crystal properties

Figure 4 reports the XRD spectra of the TiO_2NPs which displayed tetragonal crystal system. Which was confirmed by diffraction peaks at 32 ^{0}, 35 ^{0}, 37 ^{0}, 47 ^{0}, 57 ^{0}, 64 ^{0}, 68 ^{0} and 69 ^{0} in the spectra observed which corresponds to the miller indices of (100), (002), (101), (102), (110), (103), (112) and (201) respectively. XRD spectra of the TiO_2NPs display tetragonal crystal system with dominant peak at (101)

corresponding to 37 ^{0}. The observed dominant peak (101) concurred with what is reported elsewhere in the literature [36, 37]. XRD patterns showed the preferred crystal orientation of TiO_2 tetragonal crystal structure. The XRD qualities of this synthesized nanoparticles were compared with x-ray diffraction pattern of TiO_2NPs reported in literature [38-40]. The quality of TiO_2NPs is high. The sharpness of the waveform of XRD spectra indicated high crystallinity nanoparticles. Crystallite size has been estimated from XRD pattern based on the Debye- Scherer's equation [3, 41]. The average crystallite size is the nanometer range.

$$d = \frac{k\lambda}{\beta \cos\theta} \quad (3)$$

Where d is the average crystallite size, K is the Scherer constant, λ is the wavelength of radiation, β is the FWHM full width at half maximum of the diffraction peak (measured in degree), and θ is in Bragg's angle.

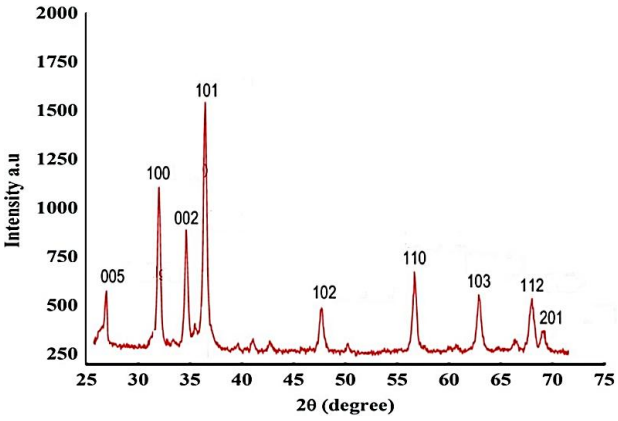


Fig. 4. XRD pattern for TiO_2NPs.

3.4 Surface morphological analysis of TiO_2NPs

Scanning Electron Microscope was used to investigate the surface characteristics of synthesized TiO_2 nanoparticles. Surface morphology of TiO_2NPs is shown in figures 5a and 5b after being annealed at 500 °C. TiO_2NPs surface morphology images observed shows high porosity due to increase in the crystal size as a result of annealing and have large grain size [42, 43]. The surface morphology of TiO_2NPs is spherical in shape and in accordance to reported literature [44, 45]. The SEM images show grain size in the nanometer range.

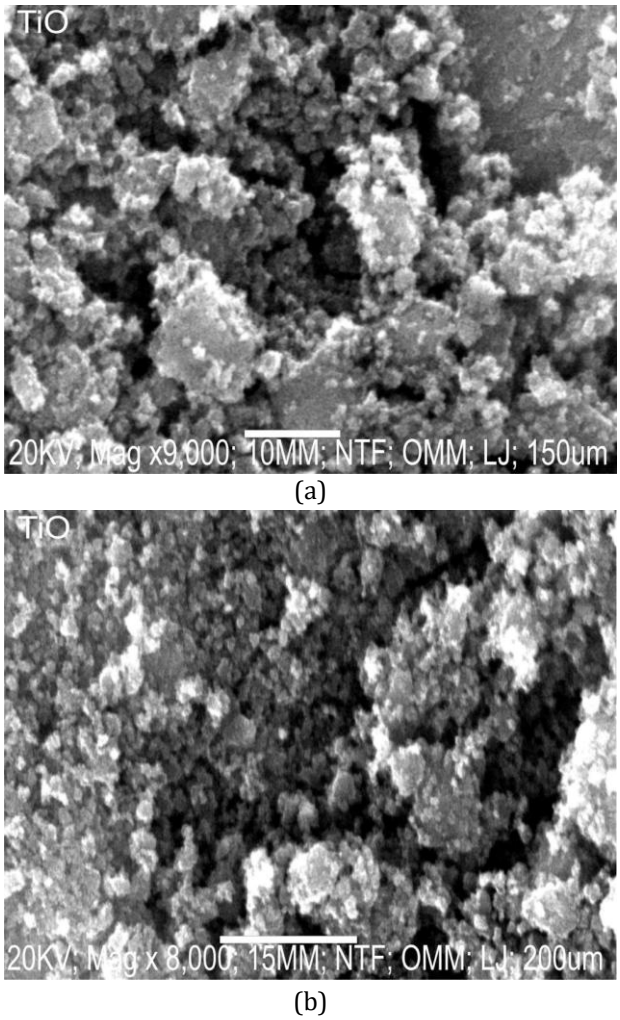


Fig. 5. SEM images of Synthesized TiO_2NPs.

3.5 Transmission electron microscopy analysis (TEM)

Figure 6 shows TEM image of TiO_2NPs. TEM images shows the grain size is spherical in shape and in the nanometer range. The result obtained in nanometer range is in agreement with SEM gain size.

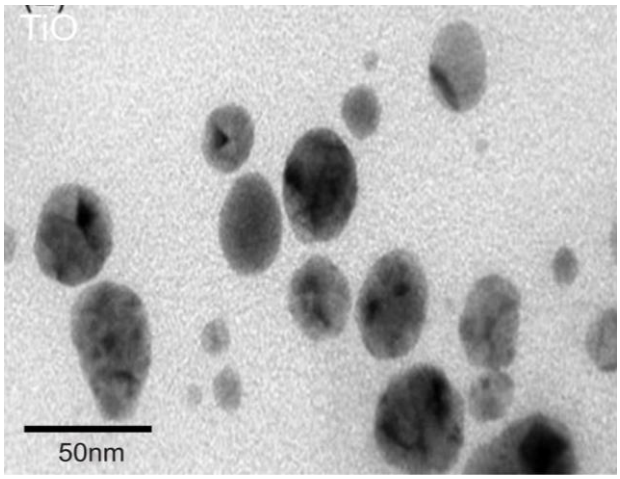


Fig. 6. TEM Image of TiO_2NPs.

3.6 Electron dispersive X-rays elemental composition analysis

EDX was utilized to determine the elemental composition of the prepared titanium dioxide nanoparticles and the purity. The elemental composition of TiO_2NPs is as analysed in figure 7. The spectrum revealed the presence of Ti and oxygen (O) at higher weight percentage confirmed formation of TiO_2NPs which concur with FTIR result and XRD.

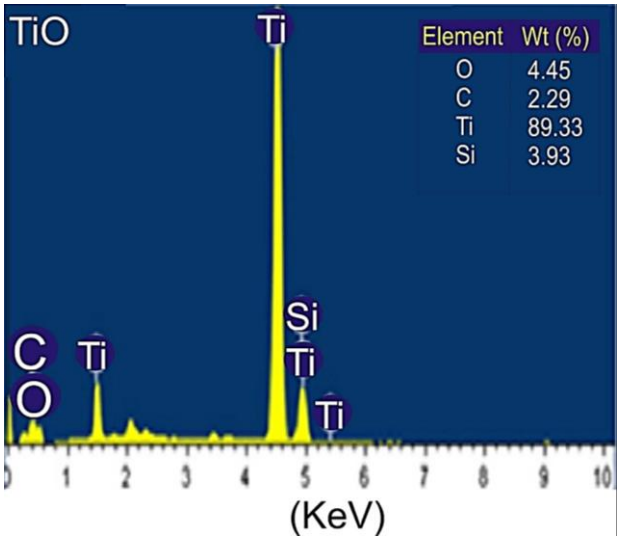


Fig. 7. EDX Spectrum of Elemental Composition of TiO_2NPs.

3.7 Electrical properties

Current-voltage characteristics for TiO_2NPs film were performed using four point probe (4PP) system equipped with Keithley2400 source measurement unit to determine electrical properties. The synthesized TiO_2NPs had been annealed at 500 °C. Figure 8 shows I-V characteristics graph of synthesized TiO_2NPs. Computation of sheet resistance was done using Eq. (4).

$$R_s = \frac{V}{I} \quad (4)$$

Where ρ= Resistivity, R= Resistance, A = Area of the glass substrate, L =length of the glass substrate. The resistivity was conducted using Eq. (5) and conductivity (σ) was computed using Eq. (6)

$$\rho = \frac{RA}{l} \quad (5)$$

$$\sigma = \frac{1}{\rho} \quad (6)$$

Table 1. Tabulated electrical properties parameters obtained for the synthesized TiO_2NPs film with average sheet resistance (R_S), resistivity (ρ) and Conductivity (σ) obtained for the synthesized TiO_2NPs film.

Sheet resistance (R_S) Ω	Resistivity (ρ) (Ωm^{-1})	Conductivity (σ) (Sm^{-1})
$67.22 * 10^6$	$1.71 * 10^6$	$0.585 * 10^{-6}$

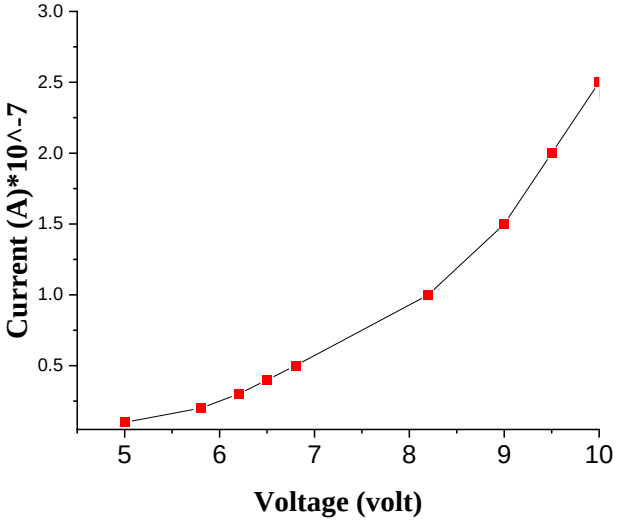


Fig. 8. I-V characteristics for TiO_2NPs thin film deposited on glass substrate.

4. CONCLUSION

A research study was conducted to investigate the use of Ixora coccinea flower extract for the biosynthesis of titanium dioxide nanoparticles. The green synthesis method using extracts offers a more eco-friendly, cost-effective, and feasible alternative to traditional synthesis methods, bridging the gap between nanotechnology and sustainability. The TiO_2 nanoparticle samples were thoroughly characterized to evaluate their properties for use as an electron transport layer. The results indicated that TiO_2NPs absorbed the highest amount of photon energy at 200 nm to 300 nm in the solar spectrum. The formation of TiO_2NPs was confirmed through FTIR testing, while the XRD spectra displayed a tetragonal crystal system with the dominant peak at (101) corresponding to 37^0. The quality of the TiO_2NPs was high, with sharp waveforms indicating high crystallinity. Electrical properties obtained included sheet resistance, resistivity, and conductivity, with values of $67.22 * 10^6$ Ω, $1.71 * 10^6$ Ωm^{-1}, and $0.585 * 10^{-6}$ Sm^{-1}, respectively. These values demonstrated better photovoltaic characteristics than bulk titanium dioxide in its pure state. The synthesized TiO_2 nanoparticles

have promising potential for use as an electron transport layer in solar cells. However, further research is recommended to test their performance in actual polymer solar cells, with a focus on solar cell parameters such as fill factors, power conversion efficiencies, and long-term performance, using synthesized TiO_2 nanoparticles on glass substrates.

Acknowledgment

This research was supported by fund. The authors are grateful to Materials Science & Engineering for the logistic support.

REFERENCES

[1] X. Wu, "Applications of titanium dioxide materials," in *IntechOpen eBooks*, 2022. doi: 10.5772/intechopen.99255.

[2] X. Chen and A. Selloni, "Introduction: Titanium Dioxide (TiO_2) Nanomaterials," *Chemical Reviews*, vol. 114, no. 19, pp. 9281–9282, Oct. 2014, doi: 10.1021/cr500422r.

[3] A. J. Haider, Z. N. Jameel, and I. H. M. Al-Hussaini, "Review on: Titanium dioxide Applications," *Energy Procedia*, vol. 157, pp. 17–29, Jan. 2019, doi: 10.1016/j.egypro.2018.11.159.

[4] U. Diebold, "The surface science of titanium dioxide," *Surface Science Reports*, vol. 48, no. 5–8, pp. 53–229, Jan. 2003, doi: 10.1016/s0167-5729(02)00100-0.

[5] G. A. Illarionov, S. M. Morozova, V. V. Chrishtop, M.-A. Einarsrud, and M. I. Morozov, "Memristive TIO_2: Synthesis, technologies, and applications," *Frontiers in Chemistry*, vol. 8, Oct. 2020, doi: 10.3389/fchem.2020.00724.

[6] S. Yekinni, I. Asiata, O. Hakeem, and L. Mubarak, "Solar photovoltaic energy system," in *IntechOpen eBooks*, 2023. doi: 10.5772/intechopen.108958.

[7] T. Pushpamalini, M. Keerthana, R. Sangavi, A. Nagaraj, and P. Kamaraj, "Comparative analysis of green synthesis of TiO_2 nanoparticles using four different leaf extract," *Materials Today: Proceedings*, vol. 40, pp. S180–S184, Jan. 2021, doi: 10.1016/j.matpr.2020.08.438.

[8] A. Saxena, R.M. Tripathi, R.P. Singh, "Biological synthesis of silver nanoparticles by using onion (allium cepa) extract and their antibacterial activity," *Digest journal of nanomaterials and biostructure*s, vol. 5, pp. 427-432, 2010.

[9] G. Sharmila et al., "Biosynthesis, characterization, and antibacterial activity of zinc oxide nanoparticles derived from Bauhinia tomentosa leaf extract," *Journal of Nanostructure in Chemistry*, vol. 8, no. 3, pp. 293–299, Jul. 2018, doi: 10.1007/s40097-018-0271-8.

[10] M. Shah, D. Fawcett, S. Sharma, S. Tripathy, and G. Poinern, "Green synthesis of metallic nanoparticles via biological entities," *Materials*, vol. 8, no. 11, pp. 7278–7308, Oct. 2015, doi: 10.3390/ma8115377.

[11] V. V. Makarov et al., "'Green' nanotechnologies: Synthesis of metal nanoparticles using plants," *Acta Naturae*, vol. 6, no. 1, pp. 35–44, Mar. 2014, doi: 10.32607/20758251-2014-6-1-35-44.

[12] A. K. Jha and K. Prasad, "Green Synthesis of Silver Nanoparticles UsingCycasLeaf," *International Journal of Green Nanotechnology. Physics and Chemistry*, vol. 1, no. 2, pp. P110–P117, May 2010, doi: 10.1080/19430871003684572.

[13] S. J. Nurani, C. K.Saha, A. R. Khan, S. Masnad H. Sunny, "Silver Nanoparticles Synthesis, Properties, Applications and Future Perspectives: A Short Review," *IOSR Journal of Electrical and Electronics Engineering (IOSR-JEEE),* vol. 10, no. 1, pp. 117-126, Nov. Dec. 2015, doi: 10.9790/1676-1061117126.

[14] L. Castro, M. L. Blázquez, J. Á. Muñoz, F. G. González, and A. Ballester, "Mechanism and applications of metal nanoparticles prepared by Bio-Mediated Process," *Reviews in Advanced Sciences and Engineering*, vol. 3, no. 3, pp. 199–216, Sep. 2014, doi: 10.1166/rase.2014.1064.

[15] S. H. Gebre and M. G. Sendeku, "New frontiers in the biosynthesis of metal oxide nanoparticles and their environmental applications: an overview," *SN Applied Sciences/SN Applied Sciences*, vol. 1, no. 8, Jul. 2019, doi: 10.1007/s42452-019-0931-4.

[16] S. W. Balogun, O. O. James, Y. K. Sanusi, and O. H. Olayinka, "Green synthesis and characterization of zinc oxide nanoparticles using bashful (Mimosa pudica), leaf extract: a precursor for organic electronics applications," *SN Applied Sciences/SN Applied Sciences*, vol. 2, no. 3, Feb. 2020, doi: 10.1007/s42452-020-2127-3.

[17] P. Basnet, T. I. Chanu, D. Samanta, and S. Chatterjee, "A review on bio-synthesized zinc oxide nanoparticles using plant extracts as reductants and stabilizing agents," *Journal of Photochemistry and Photobiology. B, Biology*, vol. 183, pp. 201–221, Jun. 2018, doi: 10.1016/j.jphotobiol.2018.04.036.

[18] J. Wu, G.-R. Bai, J. A. Eastman, G. Zhou, and V. K. Vasudevan, "Synthesis of TIO_2 nanoparticles using chemical vapor condensation," *MRS Proceedings/Materials Research Society Symposia Proceedings*, vol. 879, Jan. 2005, doi: 10.1557/proc-879-z7.12.

[19] S. A. Minicante et al., "Development of an eco-protocol for seaweed chlorophylls extraction and possible applications in dye sensitized solar cells," *Journal of Physics. D, Applied Physics*, vol. 49, no. 29, p. 295601, Jun. 2016, doi: 10.1088/0022-3727/49/29/295601.

[20] Y. Amao and Y. Yamada, "Photovoltaic conversion using Zn chlorophyll derivative assembled in hydrophobic domain onto nanocrystalline TiO_2 electrode," Biosensors & Bioelectronics/Biosensors & Bioelectronics (Online), vol. 22, no. 7, pp. 1561–1565, Feb. 2007, doi: 10.1016/j.bios.2006.07.006.

[21] X.-F. Wang et al., "Effects of plant carotenoid spacers on the performance of a dye-sensitized solar cell using a chlorophyll derivative: Enhancement of photocurrent determined by one electron-oxidation potential of each carotenoid," *Chemical Physics Letters*, vol. 423, no. 4–6, pp. 470–475, Jun. 2006, doi: 10.1016/j.cplett.2006.04.008.

[22] R. Bali, N. Razak, A. Lumb, A. Harris, "The synthesis of metallic nanoparticles inside live plants," *School of Chemical and Biomolecular Engineering*, Aug. 2006. doi: 10.1109/ICONN.2006.340592.

[23] E.-Y. Ahn, S.-W. Shin, K. Kim, and Y. Park, "Facile Green Synthesis of Titanium Dioxide Nanoparticles by Upcycling Mangosteen (Garcinia mangostana) Pericarp Extract," *Nanoscale Research Letters*, vol. 17, no. 1, Mar. 2022, doi: 10.1186/s11671-022-03678-4.

[24] G. Rajakumar, A. A. Rahuman, S. M. Roopan, I.-M. Chung, K. Anbarasan, and V. Karthikeyan, "Efficacy of larvicidal activity of green synthesized titanium dioxide nanoparticles using Mangifera indica extract against blood-feeding parasites," *Parasitology Research*, vol. 114, no. 2, pp. 571–581, Nov. 2014, doi: 10.1007/s00436-014-4219-8.

[25] R. Sankar, K. Rizwana, K. S. Shivashangari, and V. Ravikumar, "Ultra-rapid photocatalytic activity of Azadirachta indica engineered colloidal titanium dioxide nanoparticles," Applied Nanoscience, vol. 5, no. 6, pp. 731–736, Nov. 2014, doi: 10.1007/s13204-014-0369-3.

[26] T. Santhoshkumar et al., "Green synthesis of titanium dioxide nanoparticles using Psidium guajava extract and its antibacterial and antioxidant properties," Asian Pacific Journal of Tropical Medicine, vol. 7, no. 12, pp. 968–976, Dec. 2014, doi: 10.1016/s1995-7645(14)60171-1.

[27] K. Parveen, V. Banse, and L. Ledwani, "Green synthesis of nanoparticles: Their advantages and disadvantages," AIP Conference Proceedings, Jan. 2016, doi: 10.1063/1.4945168.

[28] E. O. Onah et al., "Effects of annealing temperature on TiO_2 photoelectrodes of dye-sensitized solar cells using Ixora coccenia dye extract," Journal of Nanoparticle Research, vol. 23, no. 10, Oct. 2021, doi: 10.1007/s11051-021-05335-w.

[29] M. K. Ahmad, et al., "Effect of Annealing Temperatures on Surface Morphology and Electrical Properties of Titanium Dioxide Thin Films Prepared By Sol Gel Method," *Journal of Sustainable Energy and Environment,* Jan. 2010.

[30] Z. W. Zhao and B. K. Tay, "Study of nanocrystal TiO_2 thin films by thermal annealing," Journal of Electroceramics, vol. 16, no. 4, pp. 489–493, Jul. 2006, doi: 10.1007/s10832-006-9903-3.

[31] D. J. Won, C. H. Wang, H. K. Jang, and D. K. Choi, "Effects of thermally induced anatase-to-rutile phase transition in MOCVD-grown TiO_2 films on structural and optical properties," *Applied Physics. A, Materials Science & Processing*, vol. 73, no. 5, pp. 595–600, Nov. 2001, doi: 10.1007/s003390100804.

[32] J. Tauc, R. Grigorovici, and A. Vancu, "Optical properties and electronic structure of amorphous Germanium," Physica Status Solidi (B), vol. 15, no. 2, pp. 627–637, Jan. 1966, doi: 10.1002/pssb.19660150224.

[33] B. D. Viezbicke, S. Patel, B. E. Davis, and D. P. Birnie, "Evaluation of the Tauc method for optical absorption edge determination: ZnO thin films as a model system," Physica Status Solidi. B, Basic Research, vol. 252, no. 8, pp. 1700–1710, Mar. 2015, doi: 10.1002/pssb.201552007.

[34] J.I. Pankove, Optical Processes in Semiconductors. Prentice-Hall, Technology & Engineering, (1971).

[35] E. E. Mosquera, D. Herrera-Molina, and J. Diosa, "Structural and optical properties of TiO_2 nanoparticles and their photocatalytic behavior under visible light," *Ingeniería Y Competitividad Revista CientíFica Y TecnolóGica/Ingeniería Y Competitividad*, vol. 23, no. 2, p. e21310965, May 2021, doi: 10.25100/iyc.v23i2.10965.

[36] I. N. Isnaeni, N. Indriyati, N. Dedi, D. Sumiarsa, and I. Primadona, "Green synthesis of different TiO2 nanoparticle phases using mango-peel extract," *Materials Letters*, vol. 294, p. 129792, Jul. 2021, doi: 10.1016/j.matlet.2021.129792.

[37] J. M. Abisharani, S. Devikala, R. D. Kumar, M. Arthanareeswari, and P. Kamaraj, "Green synthesis of TiO_2 Nanoparticles using Cucurbita pepo seeds extract," *Materials Today: Proceedings*, vol. 14, pp. 302–307, Jan. 2019, doi: 10.1016/j.matpr.2019.04.151.

[38] M. Aravind, M. Amalanathan, and M. S. M. Mary, "Synthesis of TiO_2 nanoparticles by chemical and green synthesis methods and their multifaceted properties," *SN Applied Sciences/SN Applied Sciences*, vol. 3, no. 4, Mar. 2021, doi: 10.1007/s42452-021-04281-5.

[39] G. Nabi, W. Raza, and M. B. Tahir, "Green synthesis of TIO2 nanoparticle using cinnamon powder extract and the study of optical properties," *Journal of Inorganic and Organometallic Polymers and Materials*, vol. 30, no. 4, pp. 1425–1429, Jul. 2019, doi: 10.1007/s10904-019-01248-3.

[40] G. Nabi et al., "A review on novel Eco-Friendly Green approach to synthesis TIO_2 nanoparticles using different extracts," *Journal of Inorganic and Organometallic Polymers and Materials*, vol. 28, no. 4, pp. 1552–1564, Feb. 2018, doi: 10.1007/s10904-018-0812-0.

[41] A. L. Patterson, "The Scherrer formula for X-Ray particle size determination," *Physical Review*, vol. 56, no. 10, pp. 978–982, Nov. 1939, doi: 10.1103/physrev.56.978.

[42] S. M. Roopan et al., "Efficient phyto-synthesis and structural characterization of rutile TiO2 nanoparticles using Annona squamosa peel extract," *Spectrochimica Acta. Part a, Molecular and Biomolecular Spectroscopy*, vol. 98, pp. 86–90, Dec. 2012, doi: 10.1016/j.saa.2012.08.055.

[43] N. Venkatachalam, M. Palanichamy, and V. Murugesan, "Sol–gel preparation and characterization of nanosize TiO_2: Its photocatalytic performance," *Materials Chemistry and Physics*, vol. 104, no. 2–3, pp. 454–459, Aug. 2007, doi: 10.1016/j.matchemphys.2007.04.003.

[44] K. L. Kelly, E. Coronado, L. L. Zhao, and G. C. Schatz, "The optical properties of metal nanoparticles: the influence of size, shape, and dielectric environment," *The Journal of Physical Chemistry. B*, vol. 107, no. 3, pp. 668–677, Dec. 2002, doi: 10.1021/jp026731y.

[45] H. Yu, S. Zhang, H. Zhao, G. Will, and P. Liu, "An efficient and low-cost TiO_2 compact layer for performance improvement of dye-sensitized solar cells," Electrochimica Acta, vol. 54, no. 4, pp. 1319–1324, Jan. 2009, doi: 10.1016/j.electacta.2008.09.025.